A Mobile Channel Model for VLC and Application to Adaptive System Design

Farshad Miramirkhani, Omer Narmanlioglu, *Student Member, IEEE*, Murat Uysal, *Senior Member, IEEE*, and Erdal Panayirci, *Life Fellow, IEEE*

***Abstract*— In this letter, we propose a realistic channel model for visible light communication (VLC) assuming a mobile user. Based on non-sequential ray tracing, we first obtain channel impulse responses for each point over the user movement trajectories, and then express path loss and delay spread as a function of distance through curve fitting. Our results demonstrate large variations in received power. In system design, this necessitates the use of adaptive schemes, where transmission parameters can be selected according to channel conditions. To demonstrate the benefits of link adaptation over a mobile VLC channel, we propose an adaptive system with luminary selection and demonstrate improvements in spectral efficiency over non-adaptive systems.**

***Index Terms*— Visible light communications, ray tracing, channel modeling, adaptive transmission.**

I. Introduction

VISIBLE light communication (VLC) makes use of the omni-present light emitting diodes (LEDs) for wireless communication. New generations of LEDs can be pulsed at very high speeds which are not noticeable to the human eye. Therefore, the existing LED-based illumination infrastructure can be used as wireless access points. Such a ubiquitous wireless access technology can be used as a powerful alternative or complementary to radio-frequency counterparts.

Despite the growing literature on VLC, the number of works on channel modeling and characterization is rather limited [1]–[10]. Furthermore, most of these works [1]–[6] focus on scenarios where transmitter and receiver are located at fixed points. There are only sporadic works which consider mobility in VLC channel modeling [7]–[10]. These however build on some simplifying assumptions such as ideal Lambertian source and purely diffuse reflections. Another simplifying assumption in [7], [8], and [10] is fixed reflectance values for surface materials (i.e., wall, floor, etc). While this can be justified for infrared wavelengths, wavelength dependency should be considered for realistic channel modeling in VLC. Most works also consider empty rooms ignoring the presence of human beings, furniture or any other objects.

Manuscript received November 8, 2016; revised December 25, 2016; accepted January 8, 2017. Date of publication January 9, 2017; date of current version May 6, 2017. This work is carried out as an activity of Optical Wireless Communication Technologies Excellence Centre funded by Istanbul Development Agency (ISTKA) under Innovative Istanbul Financial Support Program 2015 (TR10/15/YNK-72 OKATEM). The statements made herein are solely the responsibility of the authors and do not reflect the views of ISTKA and/or T.R. Ministry of Development. The works of Farshad Miramirkhani and Erdal Panayirci are supported by TUBITAK Research Grant No. 113E307. The associate editor coordinating the review of this letter and approving it for publication was P. C. Sofotasios.

F. Miramirkhani, O. Narmanlioglu, and M. Uysal are with the Department of Electrical and Electronics Engineering, Ozyegin University, 34794 Istanbul, Turkey (e-mail: farshad.miramirkhani@yahoo.com).

E. Panayirci is with the Department of Electrical and Electronics Engineering, Kadir Has University, 34083 Istanbul, Turkey (e-mail: eepanay@khas.edu.tr).

Digital Object Identifier 10.1109/LCOMM.2017.2651800

In this letter, we adopt a realistic channel modeling approach which overcomes the limitations in earlier works and present a mobile VLC channel model. In our approach which has been first used in [6] for static scenarios, all types of reflections (i.e., diffuse, specular and mixed) can be taken into account. It is not limited to Lambertian source and can handle non-ideal light sources. Furthermore, since it requires relatively less computing time in comparison to conventional ray tracing approaches, a larger number of reflections can be used for better accuracy [6].

In our work, we consider a living room with multiple luminaries, furniture and human beings inside. A user with his/her cell phone in hand walks through different trajectories within the room. We first obtain channel impulse responses (CIRs) for points over these trajectories and then determine expressions for path loss and root mean square (RMS) delay spread as a function of distance. Our results demonstrate large variations in received power. In system design, this necessitates the use of link adaptation where transmission parameters can be selected according to channel conditions. To demonstrate the benefits of link adaptation over a mobile VLC channel, we propose an adaptive system with luminary selection and demonstrate improvements in spectral efficiency (SE) over non-adaptive systems.

The remainder of the letter is organized as follows. In Section II, we first summarize the channel modeling approach, then present the expressions for path loss and RMS delay spread based on the obtained CIRs. In Section III, we propose an adaptive VLC system with luminary selection based on instantaneous received signal-to-noise ratio (SNR) and present performance improvements over non-adaptive conventional system. We finally conclude in Section IV.

II. Channel Modeling

A. Modeling Approach

In this work, we follow the channel modeling approach in [6] based on ray tracing features of Zemax®. In the first step, we create a three dimensional simulation environment where we can specify the geometry of the indoor environment and integrate the CAD models of the human beings, furniture and any other object within. The reflection characteristics of the surface materials (i.e., floor, ceilings, walls, furniture, etc) and the specifications of the light sources and detectors are further provided as additional simulation inputs.

We consider a living room with a size of 6 m × 6 m × 3 m as illustrated in Fig.1.a with plaster ceiling/walls and pinewood floor. We assume that coating materials of table, chairs, couch and coffee table are respectively pinewood, pinewood, cotton and glass. Human bodies are modeled as CAD objects with different coating materials for different parts of the body.

1558-2558 © 2017 IEEE. Personal use is permitted, but republication/redistribution requires IEEE permission.
See http://www.ieee.org/publications_standards/publications/rights/index.html for more information.

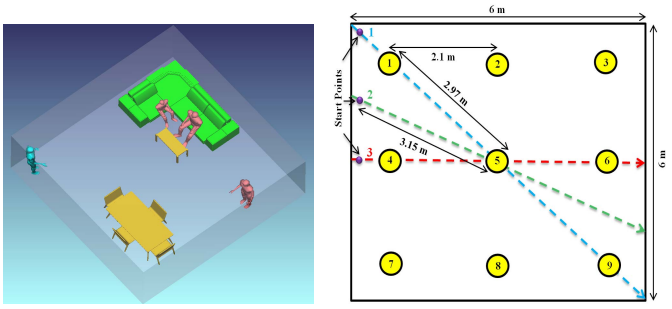

(a) (b)

Fig. 1. (a) Living room under consideration (b) movement trajectories with yellow circles denoting luminaries.

Specifically, their heads and hands are modeled as absorbing objects while cotton clothes and black gloss shoes are assumed. We assume nine luminaries on the ceiling with equidistance spacing. These are commercially available LEDs (Cree® CR6-800L) with 40° half viewing angle. The optical power for each luminary is 11 Watts. This yields an average illumination level of 153 lux which satisfies typical illumination levels for home environment [11].

Non-sequential ray tracing features of Zemax® are used to calculate the detected power and path lengths from source to detector for each ray. These are used to obtain the CIR between the light sources and each detector. The detector can be placed at any point where the CIR is desired to be computed. Here, we assume that the user walks on three different trajectories within the room (see Fig.1.b for blue, green and red lines). We assume that he/she holds a cell phone in hand next to his/her ear and the detector is located on the phone. The orientation of human body (where he/she is facing) changes according to the direction of the way while the rotation and location of cell phone (i.e., 45° rotation and at a height of 1.8 m) in his/her hand are fixed with respect to his/her ear. The field of view (FOV) and the area of the detector are 85° and 1 cm^2 respectively.

B. Path Loss and RMS Delay Spread Model

Based on the approach summarized above and given scenario, we obtain CIRs for all points with 40 cm inter-distance along each trajectory. Let $h_i(t)$ denote the individual optical CIR between the i^{th} luminary and the receiver. $h(t) = \sum_{i=1}^{N_t} h_i(t)$ represents the combined optical CIR where N_t is the number of luminaries. The path loss is given by [12]

$$PL = -10\log_{10}\left(\int_0^{\infty} h(t)\,dt\right) \tag{1}$$

and illustrated in Fig.2 for three trajectories under consideration. We apply curve fitting techniques on our observations based on the minimization of root mean square error and adopt "leave-one-out cross-validation (LOOCV)" method [13] to avoid over-fitting. The curve fitting yields

$$PL = \sum_{j=1}^{n} k_j \sin\left(l_j d + m_j\right) \tag{2}$$

where the related coefficients k_j , l_j and m_j are presented in Table I.

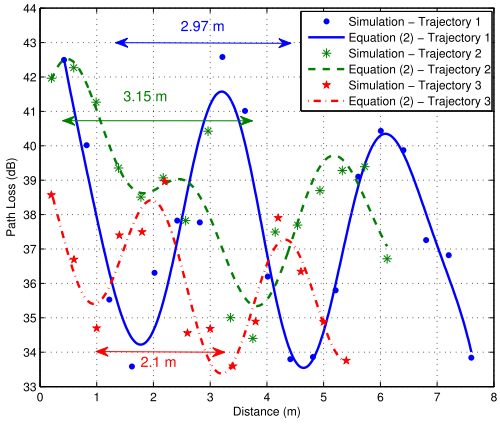

Fig. 2. Path loss vs. distance along trajectories 1, 2 and 3.

TABLE I
COEFFICIENTS IN (2) FOR ROOM WITH SIZE OF 6 m × 6 m × 3 m

Trajectory 1 (Blue Line)					
k_1	108.40	l_1	0.13	m_1	2.25
k_2	38.32	l_2	0.56	m_2	3.94
k_3	10.46	l_3	1.09	m_3	5.03
k_4	2.49	l_4	2.43	m_4	-0.08
Trajectory 2 (Green Line)					
k_1	108.90	l_1	0.40	m_1	0.28
k_2	72.22	l_2	0.52	m_2	3.00
k_3	1.35	l_3	2.67	m_3	0.64
Trajectory 3 (Red Line)					
k_1	238.00	l_1	0.24	m_1	0.59
k_2	202.80	l_2	0.27	m_2	3.62
k_3	2.05	l_3	2.76	m_3	2.25

In (2), d is the distance of user from the start point and n is given by

$$n = \begin{cases} \sqrt{N_t} + 1 & \text{for trajectory 1} \\ \sqrt{N_t} & \text{for trajectory 2 and 3} \end{cases} \tag{3}$$

It is interesting to note that the value of n is related to the number of LEDs that contribute most to received power. For example, in trajectory 1, n is equal to 4. It can be confirmed that 4 LEDs out of the total 9 contribute 95% of the total received power. Similarly, in other trajectories, a significant portion of the received power is contributed by n LEDs.

It is observed from Fig.2 that as the user moves along trajectory 1 (indicated by blue line), the received power decreases, i.e., path loss increases, as he moves away from the luminary and increases when he approaches to the next one. It can be verified that the distance of two peaks in path loss is 2.97 m which is equal to the spacing between two adjacent luminaries on that trajectory. This distance reduces to 2.1 m for trajectory 3 (indicated by red line) where three luminaries are located. Over trajectory 2 (indicated by green line), it is observed that the path loss takes its minimum value around 3.64 m where the only luminary over this trajectory (i.e., labeled as 5th LED) is located. The distance between the points where minimum and maximum path loss is 3.15 m; this corresponds to the distance of centered luminary (i.e., labeled as 5th LED) from the start point.

TABLE II
COEFFICIENTS IN (5) FOR ROOM WITH SIZE OF 6 m × 6 m × 3 m

Trajectory 1 (Blue Line)					
u_1	33.75	v_1	0.70	w_1	-1.21
u_2	38.35	v_2	1.04	w_2	0.62
u_3	37.22	v_3	1.55	w_3	1.66
u_4	23.46	v_4	1.70	w_4	4.12
Trajectory 2 (Green Line)					
u_1	31.71	v_1	0.46	w_1	0.13
u_2	20.16	v_2	0.63	w_2	2.77
u_3	0.79	v_3	3.98	w_3	-3.49
Trajectory 3 (Red Line)					
u_1	19.44	v_1	0.41	w_1	0.18
u_2	9.13	v_2	0.65	w_2	2.54
u_3	1.75	v_3	2.84	w_3	1.90

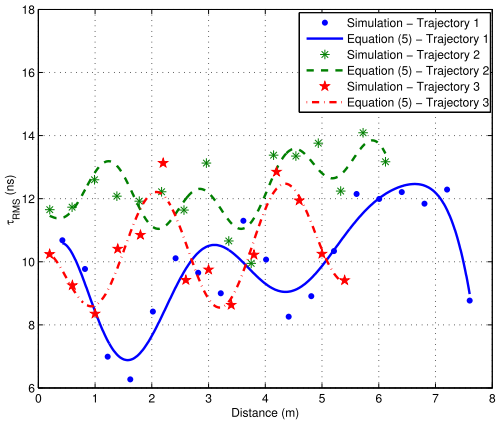

Fig. 3. RMS delay spread vs. distance along trajectories 1, 2 and 3.

The RMS delay spread of channel is defined as [6]

$$\tau_{RMS} = \sqrt{\int_0^\infty (t-\tau_0)^2 h(t)\,dt \Big/ \int_0^\infty h(t)\,dt} \qquad (4)$$

where τ_0 is the mean excess delay spread. Through curve fitting based on LOOCV method, this can be expressed as

$$\tau_{RMS} = \sum_{j=1}^{n} u_j \sin\left(v_j d + w_j\right) \qquad (5)$$

where n is given by (3) and the related coefficients u_j, v_j and w_j are presented in Table II. The RMS delay spread is illustrated in Fig.3 for three trajectories under consideration. It is observed that RMS delay spread increases when the user moves away from the luminary while it decreases when the user moves toward the luminary. This is due to the fact that the differences on the signal arrival time from the LEDs to the receiver are small when the user is close to the luminary.

To confirm the validity of (2) and (5) for different cases, we further consider two empty rooms with sizes of 9 m × 9 m × 3 m and 12 m × 12 m × 3 m. To achieve the desired illumination levels (i.e., 153 lux), we assume the deployment of 25 and 49 luminaries in a square structure with equidistant spacing. Fig.4 illustrates the path loss and RMS delay spread over the trajectory 3 for both rooms. It can be readily verified that they follow the same form as (2) and (5). The coefficients are not presented here due to space constraints.

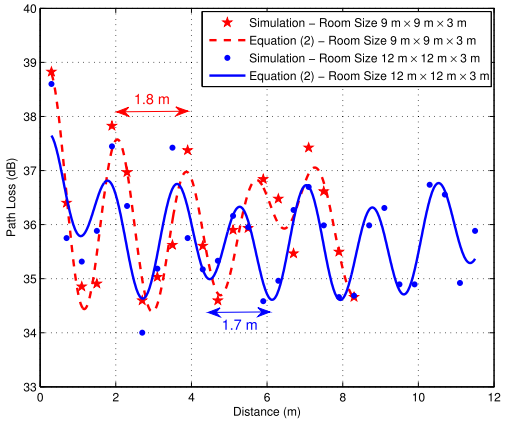

(a)

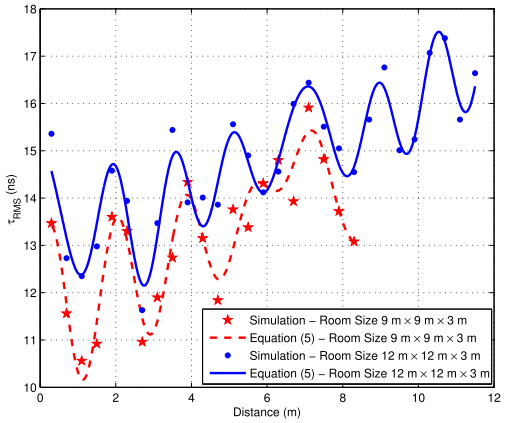

(b)

Fig. 4. (a) Path loss vs. distance (b) RMS delay spread vs. distance for rooms with sizes of 9 m × 9 m × 3 m and 12 m × 12 m × 3 m.

III. ADAPTIVE VLC SYSTEM OVER MOBILE VLC CHANNELS

As observed from Figs.2 and 4, the received power varies significantly based on the user location. Such channel dynamics necessitate the use of link adaptation [14], [15] where transmission parameters can be selected according to channel conditions. To demonstrate the benefits of link adaptation in mobile VLC channels, we propose a simple adaptive VLC transmission scheme. The proposed adaptive algorithm selects both optimal combination of LEDs and modulation order in order to maximize the signal-to-noise ratio (SNR) and spectral efficiency (SE) while satisfying a targeted value of bit error rate (BER). We assume that symbol duration is large enough so that multipath components are not resolvable and the channel acts effectively as frequency flat.[1] We use $M-$ary pulse amplitude modulation (PAM) where M is constellation size. Let us define the received SNR as

$$\text{SNR} = \frac{P}{|\Phi|\,\sigma_N^2}\left|\sum_{i\in\Phi} H_i\right|^2 \qquad (6)$$

[1]For higher data speeds where frequency-selectivity might be observed, DC-biased optical frequency division multiplexing (DCO-OFDM) can be employed.

TABLE III

REQUIRED SNR LEVELS TO SATISFY 10^{-3} BER TARGET FOR DIFFERENT MODULATIONS

Modulation	Required SNR [dB]
2−PAM	9.80
4−PAM	16.54
8−PAM	22.55
16−PAM	28.42
32−PAM	34.26
64−PAM	40.12

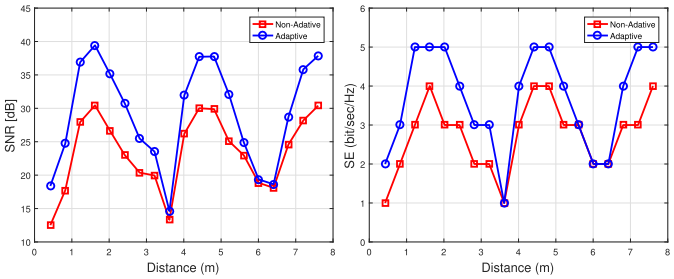

(a) (b)

Fig. 5. (a) SNR and (b) SE comparisons of non-adaptive and adaptive cases.

where P is the total information power,[2] $H_i = \int_0^\infty h_i(t)dt$, Φ is a vector including the index of active LEDs (i.e., selected for data transmission), $|\Phi|$ denotes the number of active LEDs, i.e., the length of vector Φ, and σ_N^2 is the noise power. First the selection of LEDs (i.e., which LEDs are selected to transmit data) is made to maximize the received SNR. Specifically, we first list all possible combination of LEDs. For each combination, we calculate the instantaneous SNR based on (6). Among all possible combinations, we then determine the best combination which maximizes the SNR value in (6) through brute-force search. Then, the highest modulation order that maximizes the SE is selected while satisfying a pre-determined BER. This selection can be carried out with the help of a look-up table where minimum SNR thresholds for different modulation orders to achieve the given BER target are provided. As an example, Table III summarizes required SNRs to achieve BER $= 10^{-3}$ for different sizes of PAM.

The performance of the proposed adaptive scheme is illustrated in Fig.5 in terms of received SNR and SE. The non-adaptive scheme where all nine LEDs simultaneously transmit data is used as a benchmark. It is observed that both SNR and SE are improved through adaptive LED selection. The highest SNR improvement is obtained when the user is at the distance of 1.6 m from the start point. When the user is at this particular location, the adaptive scheme suggests the use of only the 1st LED for data transmission, thereby all AC power is allocated to this LED. The SNR improvement allows the deployment of 32−PAM instead of 16−PAM that is used by the non-adaptive scheme, effectively resulting in SE increase. On the other hand, the lowest SNR improvement is observed when the user is at the distance of 6 m from the start point. At this particular case, six out of total nine LEDs are active (i.e., transmitting data). It is observed from SE plot that the SNR improvement is not enough to increase the modulation order and the performance therefore remains the same as in non-adaptive case. In between these two extremes, the number of active LEDs varies between one and six.

[2]The illumination level is determined by the DC bias value and independent of information signal power.

IV. CONCLUSIONS

In this letter, we have developed a mobile VLC channel based on non-sequential ray tracing. For realistic modeling, wavelength dependency was explicitly taken into account while different types of reflections (i.e., diffuse, specular and mixed reflections) were considered. An indoor environment with furniture and CAD human models as well as commercially available light sources were used in our simulations. Under these realistic assumptions, we have obtained CIRs over the user movement trajectories that the user moves and presented expressions for path loss and delay spread through curve fitting. Motivated by the fact that received power varies significantly based on the user location, we have further proposed an adaptive luminary selection and demonstrated improvements in spectral efficiency over non-adaptive systems.

REFERENCES

[1] H. Chun, C. J. Chiang, and D. C. O'Brien, "Visible light communication using OLEDs: Illumination and channel modeling," in *Proc. Int. Workshop Opt. Wireless Commun. (IWOW)*, Oct. 2012, pp. 1–3.

[2] H. Q. Nguyen *et al.*, "A MATLAB-based simulation program for indoor visible light communication system," in *Proc. IEEE 7th Int. Symp. Commun. Syst. Netw. Digit. Signal Process. (CSNDSP)*, Jul. 2010, pp. 537–541.

[3] T. Komine and M. Nakagawa, "Performance evaluation of visible-light wireless communication system using white led lightings," in *Proc. IEEE 9th Int. Symp. Comput. Commun.*, vol. 1, Jun. 2004, pp. 258–263.

[4] S. Long, M.-A. Khalighi, M. Wolf, S. Bourennane, and Z. Ghassemlooy, "Channel characterization for indoor visible light communications," in *Proc. IEEE 3rd Int. Workshop Opt. Wireless Commun. (IWOW)*, Sep. 2014, pp. 75–79.

[5] K. Lee, H. Park, and J. R. Barry, "Indoor channel characteristics for visible light communications," *IEEE Commun. Lett.*, vol. 15, no. 2, pp. 217–219, Feb. 2011.

[6] F. Miramirkhani and M. Uysal, "Channel modeling and characterization for visible light communications," *IEEE Photon. J.*, vol. 7, no. 6, Dec. 2015.

[7] T. Komine and M. Nakagawa, "A study of shadowing on indoor visible-light wireless communication utilizing plural white LED lightings," in *Proc. 1st Int. Symp. Wireless Commun. Syst.*, Sep. 2004, pp. 36–40.

[8] T. Komine, S. Haruyama, and M. Nakagawa, "A study of shadowing on indoor visible-light wireless communication utilizing plural white led lightings," *Wireless Pers. Commun.*, vol. 34, no. 1, pp. 211–225, Jul. 2005.

[9] Y. Xiang *et al.*, "Human shadowing effect on indoor visible light communications channel characteristics," *Opt. Eng.*, vol. 53, no. 8, p. 086113, Aug. 2014.

[10] P. Chvojka, S. Zvanovec, P. A. Haigh, and Z. Ghassemlooy, "Channel characteristics of visible light communications within dynamic indoor environment," *IEEE J. Lightw. Technol.*, vol. 33, no. 9, pp. 1719–1725, May 1, 2015.

[11] *Lighting of Indoor Work Places*, Standard ISO 8995:2002 CIE S 008/ E-2001, 2001.

[12] A. T. Hussein and J. M. H. Elmirghani, "Performance evaluation of multi-gigabit indoor visible light communication system," in *Proc. 20th Eur. Conf. Netw. Opt. Commun. (NOC)*, Jun. 2015, pp. 1–6.

[13] G. James, D. Witten, T. Hastie, and R. Tibshirani, *An Introduction to Statistical Learning*. vol. 6. New York, NY, USA: Springer, 2013.

[14] Q. Zhou and H. Dai, "Joint antenna selection and link adaptation for MIMO systems," *IEEE Trans. Veh. Technol.*, vol. 55, no. 1, pp. 243–255, Jan. 2006.

[15] N. P. Le, F. Safaei, and L. C. Tran, "Antenna selection strategies for MIMO-OFDM wireless systems: An energy efficiency perspective," *IEEE Trans. Veh. Technol.*, vol. 65, no. 4, pp. 2048–2062, Apr. 2016.